background factors between the two groups showed that there were fewer female patients and that the serum albumin level was higher in the IFN group. On the other hand, the AFP level was higher and the Japanese TNM stage was advanced in many of the non-IFN group patients (Table 1). The median follow-up period was 37 and 31 months in the IFN and non-IFN groups, respectively.

Matching was performed using the propensity score to adjust for the background factors. The ten factors, as described above, were adopted for the covariates. Twenty patients were selected from each of the IFN and non-IFN groups through this matching. The *C*-statistic was 0.756. There were no significant differences between the matched patient groups in any of the host, tumor, or viral side background factors (Table 2). The 5-year cumulative survival rates were 100 and 76.9% in the IFN and non-IFN groups, respectively. This difference was not significant ($P = 0.075$) although the rate was higher in the IFN group (Fig. 1a).

HCC recurred after RFA in eight patients in the IFN group and in 12 patients in the non-IFN group. The 1- and 3-year cumulative recurrence rates were 5.0 and 38.0%, respectively, in the IFN group, and 22.2 and 64.2%, respectively, in the non-IFN group. The lower rates in the IFN group were statistically significant ($P = 0.019$) (Fig. 1b).

The patients were classified as "IFN responders" or as "Others". IFN responders consisted of 3 SVR patients and 11 patients in whom the serum ALT level had normalized at 30 IU/mL or lower on IFN therapy (14 patients in total). The "Others" group consisted of 26 patients. The cumulative recurrence rate was analyzed in the groups. The 1- and 3-year cumulative recurrence rates were 0 and 29.3%, respectively, in the IFN responders group and 20.7 and 63.7%, respectively, in the "Others" group. The lower rates in the IFN responders were statistically significant ($P = 0.001$; Fig. 2). The hazards ratio for recurrence in the IFN responders, based on the Cox proportional hazards model, was 0.158 (95% confidence interval = 0.045-0.561, $P = 0.004$). Local tumor progression was noted in three patients from the "Others" group, and in one patient of the IFN responders ($P = 0.45$; Fig. 3a). The cumulative ectopic recurrence rate was significantly lower in the IFN responders than in the "Others" group ($P = 0.008$; Fig. 3b).

Changes in the serum albumin level were also investigated. The difference between the level immediately before RFA and that measured for data analysis were compared between the two groups. The median duration of the measurement period was 21 and 17 months in the IFN responders and "Others" group, respectively. This difference was not statistically significant ($P = 0.08$). The serum albumin level was retained in the IFN responders, but decreased in the "Others" group ($P = 0.001$; Fig. 4).

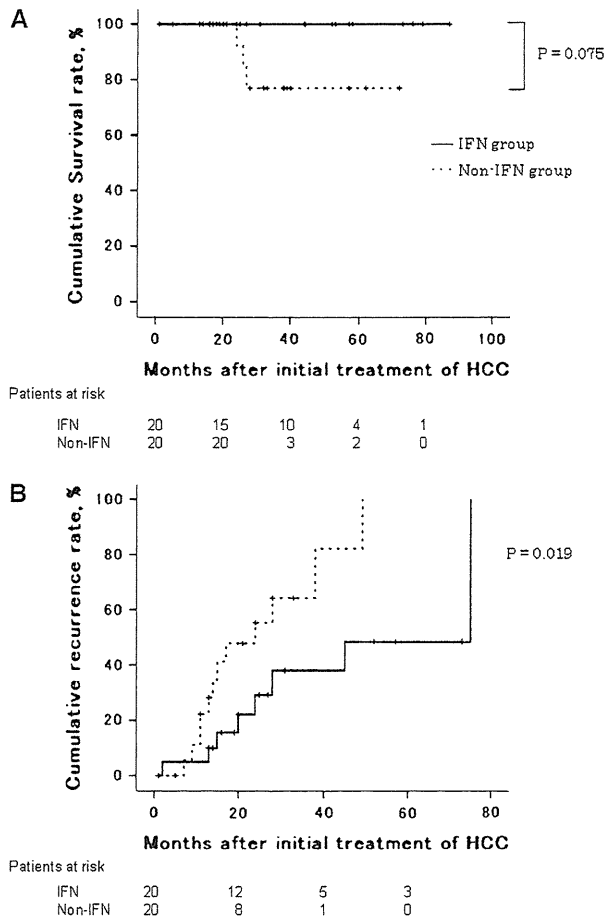

Fig. 1 **a** Cumulative survival rates after curative RFA treatment of matched patients with HCC. The cumulative rates were higher in the IFN group than in the non-IFN group ($P = 0.075$). **b** Cumulative recurrence rates after RFA treatment of matched patients with HCC. The recurrence rate of the IFN group was significantly lower than that of the non-IFN group ($P = 0.019$)

Discussion

The mechanism of HCV-associated carcinogenesis has been actively investigated, but it has not been fully elucidated [21]. Therapy for HCC has had marked advancements in recent years. However, this has not sufficiently increased the long-term survival rate. The annual recurrence rate of HCC is as high as 10–25%, even after curative treatment [22, 23]. In many patients, the background liver disease is hepatic cirrhosis, which gradually progresses to liver failure. Advances in treatment methods and determining how to inhibit recurrence are important in improving the prognosis of HCC. The usefulness of IFN therapy as a primary prevention of chronic hepatitis C and hepatic cirrhosis is well-recognized in Japan. IFN therapy apparently inhibits carcinogenesis in patients who achieve SVR [5–9]. We previously reported IFN's carcinogenesis-inhibitory effect

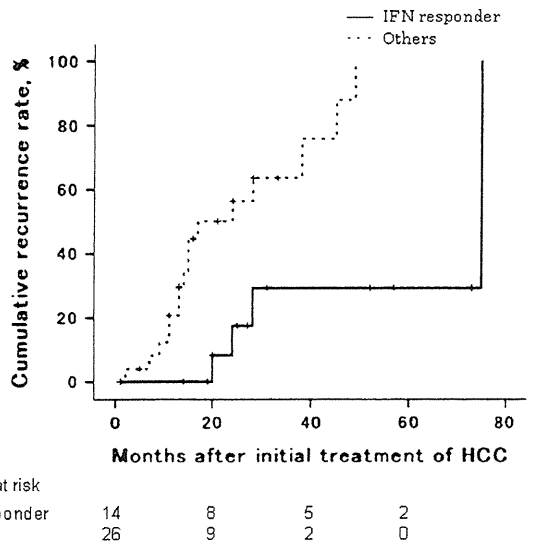

Fig. 2 Cumulative recurrence rates according to efficacy of IFN therapy after curative RFA treatment of matched patients with HCC. The rate of cumulative recurrence of HCC in the IFN responder was significantly lower than the "Others" ($P = 0.001$)

on HCV-induced hepatic cirrhosis [5, 6]. Many clinical studies, mainly in Japan, have confirmed this effect [7–9]. In this study, we performed matching using the propensity score since we noted biases in the background factors between the IFN and non-IFN groups. This method is used in many fields as a covariate adjustment method and modifies the dependent variables in observational studies in which randomized allocation is difficult [24, 25]. The *C*-statistic was 0.756, showing a favorable matching.

In the matched groups, the cumulative survival rate was higher in the IFN group while the cumulative recurrence rate in this group was significantly lower. IFN exhibited an anti-viral effect, in addition to inhibiting liver cancer cell growth, in a basic study [26]. It also has a clinical anti-tumor effect on HCC [27, 28]. Ikeda et al. [10] and Kubo et al. [11] reported the efficacy of IFN-β and IFN-α, respectively, in inhibiting carcinogenesis after the curative treatment of HCC. Shiratori et al. [12] noted that IFN does not inhibit the initial recurrence of HCC, but it does inhibit subsequent recurrences. We performed long-term IFN monotherapy and prolonged IFN therapy by adding IFN monotherapy after PEG-IFN/RBV combination therapy. This suggests that IFN therapy is useful as a secondary prevention of carcinogenesis. However, the number of patients we used was small. Previous basic study has shown that continuous IFN administration induces anti-tumor effects [29]. Kudo et al. [15] also performed maintenance IFN therapy for HCC after RFA. In their study, the anti-tumor and the carcinogenesis-inhibitory effect of IFN therapy inhibited HCC recurrence and improved treatment outcomes.

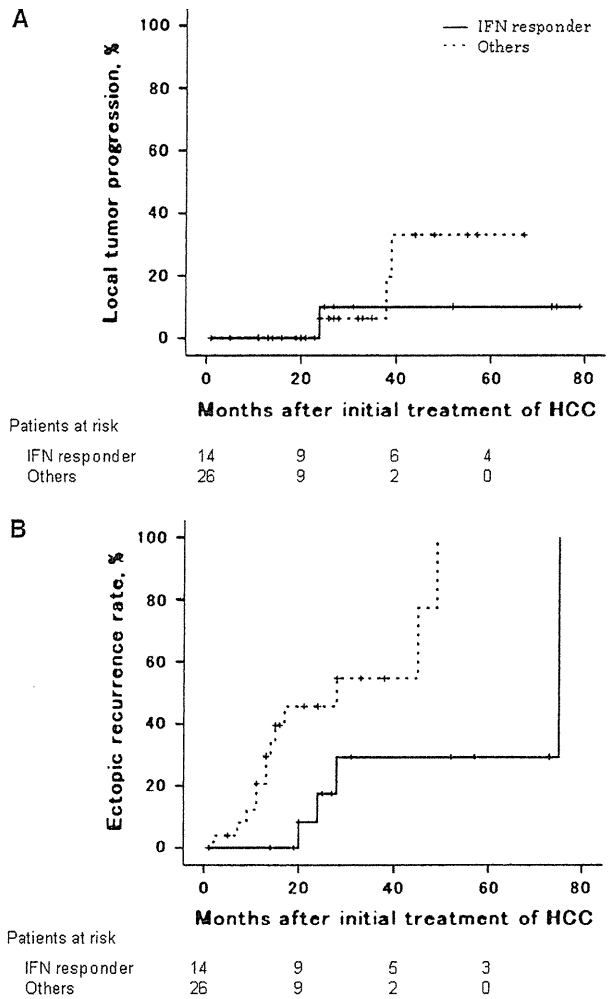

Fig. 3 Cumulative recurence rates after RFA treatment of matched patients with HCC. **a** Rates of local tumor progression was lower than that of the "Others", but the difference was not statistically significant ($P = 0.45$). **b** Rates of ectopic recurrence of the IFN responder was significantly lower than that of the "Others" ($P = 0.002$)

An analysis of the IFN responder patients and the "Others" groups shows that the IFN-induced reduction of the serum ALT level to 30 IU/mL or lower may be important for inhibiting intrahepatic recurrence. Yoshida et al. [7] performed IFN therapy in patients with chronic type C hepatitis and observed a carcinogenesis-inhibitory effect in biological responders. This was similar to the effect in the SVR patients. Wang et al. [30] reported that high-dose and long-term therapy with IFN-α inhibited intrahepatic tumor recurrence and lung metastasis in nude mice after curative resection. Uenishi et al. [31] performed IFN therapy after surgery for HCC and observed a recurrence-inhibitory effect in patients in whom the serum ALT level normalized, regardless of disappearance of serum HCV RNA. We also observed a low ectopic recurrence rate in the IFN responders. Recent studies of meta-analysis

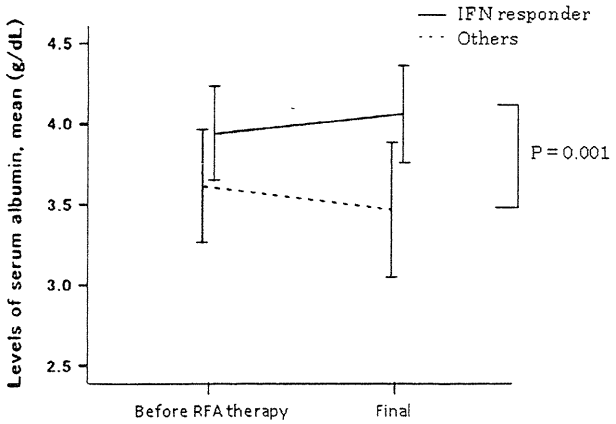

Fig. 4 Effect of IFN therapy after curative RFA treatment of matched patients with HCC on the levels of serum albumn. The *bars* indicate mean ± 1 SD. Serum albumin in the IFN responders was significantly better preserved than the "Others" ($P = 0.001$)

have shown that IFN-α treatment could significantly decrease early recurrence, so-called intrahepatic metastasis, and improved 1-year survival of patients with HCC after complete resection or ablation [32, 33]. This study suggests that IFN therapy is effective for the suppression of intrahepatic metastasis of HCC. This effect of IFN might be related with the direct suppression of tumor growth on an already-existing undetectable malignant lesion. However, mechanisms of IFN's effect on recurrence were very complex so that no single study could explain them fully.

Jeong et al. [14] reported maintenance of the Child-Pugh score in patients in whom IFN therapy achieved SVR after curative treatment of HCV-associated HCC. This study suggested that the improvement in and the maintenance of the serum albumin level (an important index of liver function) contributed to improved treatment outcomes. In other words, the recurrence is inhibited and liver function is improved in the IFN responders after HCC treatment. This indicates that curative treatment can be performed, even if recurrence occurs. The statistical method used to adjust for the background factors indicated that long-term IFN administration for HCC after RFA inhibited recurrence and improved the treatment outcome—particularly in the IFN responders.

There are several problems with IFN therapy. It is not applicable to patients with a poor liver function. Diverse adverse effects appear with the therapy such as thrombocytopenia. These problems need to be considered in reaching a conclusion concerning IFN administration to prevent recurrence after the curative treatment of HCC. A large-scale prospective study is needed that covers the type and dose of IFN, use of concomitant drugs (such as ribavirin), and the duration of IFN administration.

References

1. Hashem B, Lenhard R. Hepatocellular carcinoma: epidemiology and molecular carcinogenesis. Gastroenterology 2007;132: 2557–2576
2. Koike K, Tsutsumi T, Fujie H, Shintani Y, Moriya K. Molecular mechanism of viral hepatocarcinogenesis. Oncology 2002;62 (Suppl 19):29–37
3. Imamura H, Matsuyama Y, Tanaka E, Ohkubo T, Hasegawa K, Miyagawa S, Sugawara Y, Minagawa M, Takayama T, Kawasaki S, Makuuchi M. Risk factor contributing to early and late phase intrahepatic recurrence of hepatocellular carcinoma after hepatectomy. J Hepatol 2003;38:200–203
4. Ikeda K, Arase Y, Kobayashi M, Saitoh S, Someya T, Hosaka T, Suzuki Y, Suzuki F, Tsubota A, Akuta N, Kumada H. Significance of multicentric cancer recurrence after potentially curative ablation of hepatocellular carcinoma: a longterm cohort study of 892 patients with viral cirrhosis. J Gastroenterol 2003;38: 865–876
5. Nishiguchi S, Kuroki T, Nakatani S, Morimoto H, Takeda T, Nakajima S, Shiomi S, Seki S, Kobayashi K, Otani S. Randomised trial of effects of Interferon-α on incidence of hepatocellular carcinoma in chronic active hepatitis C with cirrhosis. Lancet 1995;346:1051–1055
6. Nishiguchi S, Shiomi S, Nakatani S, Takeda T, Fukuda K, Tamori A, Habu D, Tanaka T. Prevention of hepatocellular carcinoma in patients with chronic active hepatitis C and cirrhosis. Lancet 2001;357:196–197
7. Yoshida H, Arakawa Y, Sata M, Nishiguchi S, Yano M, Fujiyama S, Yamada G, Yokosuka O, Shiratori Y, Omata M. Interferon therapy prolonged life expectancy among chronic hepatitis C patients. Gastroenterology 2002;123:483–491
8. Shiratori Y, Ito Y, Yokosuka O, Imazeki F, Nakata R, Tanaka N, Arakawa Y, Hashimoto E, Hirata K, Yoshida H, Ohashi Y, Omata M. Antiviral therapy for cirrhotic hepatitis C: association with reduced hepatocellular carcinoma development and improved survival. Ann Intern Med 2005;142:105–114
9. Kurokawa M, Hiramatsu N, Oze T, Mochizuki K, Yakushijin T, Kurashige N, Inoue Y, Igura T, Imanaka K, Yamada A, Oshita M, Hagiwara H, Ito T, Inui Y, Hijioka T, Yoshihara H, Inoue A, Imai Y, Kato M, Kiso S, Kanto T, Takehara T, Kasahara A, Hayashi N. Effect of interferon α-2b plus ribavirin therapy on incidence of hepatocellular carcinoma in patients with chronic hepatitis. Hepatol Res 2009;39:432–438
10. Ikeda K, Arase Y, Saitoh S, Kobayashi M, Suzuki Y, Suzuki F, Tsubota A, Chayama K, Murashima N, Kumada H. Interferon beta prevents recurrence of hepatocellular carcinoma after complete resection or ablation of the primary tumora prospective randomized study of hepatitis C virus-related liver cancer. Hepatology 2000;32:228–232
11. Kubo S, Nishiguchi S, Hirohashi K, Tanaka H, Shuto T, Kinoshita H. Randomized clinical trial of long-term outcome after resection of hepatitis C virus-related hapatocellular carcinoma by postoperative interferon therapy. Br J Surg 2002;89:418–422
12. Shiratori Y, Shiina S, Teratani T, Imamura M, Obi S, Sato S, Koike Y, Yoshida H, Omata M. Interferon therapy after tumor ablation improves prognosis in patients with hepatocellular carcinoma associated with hepatitis C virus. Ann Intern Med 2003;138:299–306
13. Nishiguchi S, Tamori A, Kubo S. Effect of long-term postoperative interferon therapy on intrahepatic recurrence and survival rate after resection of hepatitis C virus-related hepatocellular carcinoma. Intervirology 2005;48:71–75
14. Jeong SC, Aikata H, Katamura Y, Azakami T, Kuwaoka T, Saneto H, Uka K, Mori N, Takaki S, Kodama H, Waki K,

Imamura M, Shirakawa H, Kawakami Y, Takahashi S, Chayama K. Effects of a 24-week course of interferon-α therapy after curative treatment of hepatitis C virus- associated hepatocellular carcinoma. World J Gastroenterol 2007;13:5343–5350
15. Kudo M, Sakaguchi Y, Chung H, Hatanaka K, Hagiwara S, Ishikawa E, Takahashi S, Kitai S, Inoue T, Minami Y, Ueshima K. Long-term interferon maintenance therapy improves survival in patients with hepatitis C virus-related hepatocellular carcinoma after curative radiofrequency ablation. Oncology 2007;72(Suppl 1):132–138
16. Mazzaferro V, Romito R, Schiavo M, Mariani L, Camerini T, Bhoori S, Capussotti L, Calise F, Pellicci R, Belli G, Tagger A, Colombo M, Bonino F, Majno P, Liovet JM. Prevention of hepatocellular carcinoma recurrence with alpha-interferon after liver resection in hepatitis C virus cirrhosis. Hepatology 2006;44:1543–1554
17. Rosenbaum PR, Rubin DB. The central role of the propensity score in observational studies for causal effects. Biometrika 1983;70:41–55
18. D'Agostino RB Jr. Propensity score methods for bias reduction in the comparison of a treatment to a non-randomized control group. Stat Med 1998;17:2265–2281
19. Minagawa M, Ikai I, Matsuyama Y, Yamaoka Y, Makuuchi M. Staging of hepatocellular carcinoma: assessment of the Japanese Tumor-Node-Metastasis and American Joint Committee on Cancer/International Union Against Cancer Tumor-Node-Metastasis systems in a cohort of 13,772 patients in Japan. Ann Surg 2007;245:909–922
20. Weitzen S, Lapane KL, Toledano AY, Hume AL, Mor V. Weaknesses of goodness-of-fit tests for evaluating propensity score models. Pharmacoepidemiol Drug Saf 2005;14:227–238
21. Koike K. Pathogenesis of hepatitis C virus-associated hepatocellular carcinoma: dual-pass carcinogenesis through activation of oxidative stress and intracellular signaling. Hepatol Res 2007;37:115–120
22. Kumada T, Nakano S, Takeda I, Sugiyama K, Osada T, Kiriyama S, Sone Y, Toyoda H, Shimada S, Takahashi M, Sassa T. Pattern of recurrence after initial treatment in patients with small hepatocellular carcinoma. Hepatology 1997;25:87–92
23. Tsukuma H, Hiyama T, Tanaka S, Nakao M, Yabuubhi T, Kitamura T, Nakanishi K, Fujimoto I, Inoue A, Yamazaki H, Kawashima T. Risk factors for hepatocellular carcinoma among patients with chronic liver disease. N Engl J Med 1993;328:1797–1801
24. Iwashyna TJ, Lamont EB. Effectiveness of adjuvant fluorouracil in clinical practice: a population-based cohort study of elderly patients with stage III colon cancer. J Clin Oncol 2002;20: 3992–3998
25. Wang PS, Schneeweiss S, Avorn J, Fischer MA, Mogun H, Solomon DH, Brookhart MA. Risk of death in elderly users of conventional versus atypical antipsychotic medications. N Engl J Med 2005;353:2335–2341
26. Yano H, Iemura A, Haramaki M, Ogasawara S, Takayama A, Akiba J, Kojiro M. Interferon alfa receptor expression and growth inhibition by interferon alfa in human liver cancer cell lines. Hepatology 1999;29:1708–1717
27. Lai CL, Lau JY, Wu PC, Ngan H, Chung HT, Mitchell S, Corbett TJ, Chow AW, Lin HJ. Recombinant interferon-alpha in inoperable hepatocellular carcinoma: a randomized controlled trial. Hepatology 1993;17:389–394
28. Ota H, Nagano H, Sakon M, Eguchi H, Kondo M, Yamamoto T, Nakamura M, Damdinsuren B, Wada H, Marubashi S, Miyamoto A, Done K, Umeshita K, Nakamori S, Wakasa K, Monden M. Treatment of hepatocellular carcinoma with major portal vein thrombosis by combination of subcutaneous interferon-α and intraarterial 5-fluorouracil: role of expression of type 1 interferon receptor. Br J Cancer 2005;93:557–564
29. Yano H, Ogasawara S, Momosaki S, Akiba J, Kojiro S, Fukahori S, Ishizaki H, Kuratomi K, Basaki Y, Oie S, Kuwano M, Kojiro M. Growth inhibitory effects of pegylated interferon alpha-2b on human liver cancer cells in vitro and in vivo. Liver Int 2006;26: 964–975
30. Wang L, Tang ZY, Qin LX, Wu XF, Sun HC, Xue Q, Ye SL. High-dose and long-term therapy with interferon-alfa inhibits tumor growth and recurrence in nude mice bearing human hepatocellular carcinoma xenografts with high metastatic potential. Hepatology 2000;32:43–48
31. Uenishi T, Nishiguchi S, Tamori A, Yamamoto T, Shuto T, Hirohashi K, Takemura S, Tanaka H, Kubo S. Influence of interferon therapy on outcome after surgery for hepatitis C virus-related hepatocellular carcinoma. Hepatol Res 2006;36:195–200
32. Zhang CH, Xu GL, Jia WD, Ge YS. Effects of interferon alpha treatment on recurrence and survival after complete resection or ablation of hepatocellular carcinoma: a meta-analysis of randomized controlled trials. Int J Cancer 2009;124:2982–2988
33. Shen YC, Hsu C, Chen LT, Cheng CC, Hu FC, Cheng AL. Adjuvant interferon therapy after curative therapy for hepatocellular carcinoma (HCC): a meta-regression approach. J Hepatol 2010;52:889–894

Trends in Cancer Research
Vol. 5, 2009

Original Communication

A higher expression of hepatoma-derived growth factor in hepatocellular carcinoma cells and more tumor growth *in vivo*

Weidong Liu, Hideji Nakamura*, Hong Deng, Hirayuki Enomoto, Teruhisa Yamamoto, Yoshinori Iwata, Noritoshi Koh, Masaki Saito, Hiroyasu Imanishi, Soji Shimomura, and Shuhei Nishiguchi

Division of Hepatobiliary and Pancreatic Medicine, Department of Internal Medicine, Hyogo College of Medicine, Mukogawa-cho 1-1, Nishinomiya, Hyogo 663-8501, Japan

ABSTRACT

Hepatoma-derived growth factor (HDGF) is a unique nuclear targeting growth factor which plays an important role in both carcinogenesis and cancer progression. Exogenously supplied and endogenously over-expressed HDGF stimulates the proliferation of hepatocellular carcinoma (HCC) cells. In the present study, to clarify the effects of HDGF on HCC, HDGF over-expressing cells were cloned and their biological functions for the growth of HCC were investigated. An anchorage-independent colony formation assay, xenograft tumor formation experiment and a DNA chip analysis were all performed. In a human HCC cell line, HepG2 cells over-expressing HDGF (HepG2-HDGF) proliferate more rapidly than mock HepG2 (HepG2-neo) cells *in vitro*. According to an anchorage independent colony assay, HepG2-HDGF cells formed more and bigger colonies than HepG2-neo in soft agar. HepG2-HDGF cells generate tumors earlier and promote tumor growth more rapidly than HepG2-neo cells in nude mice. The tumors which develop from HepG2-HDGF cells show a more reddish color macroscopically and a richer in vasculature microscopically than the tumors from HepG2-neo cells. According to the DNA-chip analyses, both *in vitro* and *in vivo* up-regulated genes due to HDGF over-expression are demonstrated, including PDGF-A, matrix metalloproteinase-1, urokinase-type plasminogen activator, chitinase 3-like-2 and ankyrin, which are related to tumor growth and aggressive characteristics. These findings suggest that HDGF enhance tumor growth while also inducing the aggressive biological functions, through the expression of genes which are related to invasion, metastasis and angiogenesis *in vivo*. Therefore, HDGF is considered to play an important role in the progression of HCC as well as hepatocarcinogenesis.

KEYWORDS: HDGF, tumor, angiogenesis

INTRODUCTION

Hepatoma-derived growth factor (HDGF) is a heparin-binding growth factor, which has a mitogenic function on fibroblasts, smooth muscle cells, endothelial cells and hepatoma cells [1-7]. The trafficking to the nucleus is important to exert the mitogenic activity, and HDGF belongs to the group of the nuclear targeting growth factor [5, 6]. The down regulation of HDGF by anti-sense oligonucleotides and small interfering RNAs (siRNA) suppressed the proliferation of cancer cells [8, 9]. Furthermore, exogenously supplied HDGF stimulated the DNA synthesis and cellular proliferation of several cells including cancer cells, although its receptor has not yet been identified.

*Corresponding author
nakamura@hyo-med.ac.jp

HDGF is not only highly expressed in a large number of different tumor types such as hepatocellular carcinoma (HCC), non-small cell lung cancer (NSCLC), and gastric adenocarcinoma, but it is also related to tumor invasion, metastasis and recurrence [10-17]. HDGF expression has been induced in the liver at a stage before HCC development, and it thereafter gradually increases during tumor growth in a rat hepatocarcinogenesis model [10]. Furthermore, HDGF has both an angiogenic activity as well as a cell growth stimulating activity [7, 18]. HDGF therefore appears to be a novel prognostic factor for patients suffering from different types of cancer [11-14, 16, 19-21]. HDGF is considered to be closely linked to carcinogenesis and the aggressive biological potential of tumor cells *in vivo*. However, the role of HDGF on HCC biology *in vivo* remains to be elucidated.

Previously we reported that HDGF over-expression in NIH3T3 induced a significant tumor formation in nude mice [7]. In the present study, HDGF over-expressing HepG2 cells were cloned and their biological functions for tumor growth were investigated by the use of an anchorage-independent colony formation assay in soft agar, xenograft tumor formation experiments and a DNA chip gene analysis.

MATERIALS AND METHODS

Anchorage-independent growth assay in soft agar

HDGF stably over-expressing HepG2 (HepG2-HDGF) and mock HepG2 (HepG2-neo) cells were established and maintained as reported previously [6]. The expression of myc-tagged HDGF and native HDGF was confirmed by Western blotting using polyclonal anti-C terminus of HDGF antibody at a dilution of 1 x 10,000.

To assess the anchorage independency of growth, 5,000 cells in 1.5 ml of 0.35% agar with DMEM were plated in each well on the top of an existing 0.5% bottom agar-DMEM in six-well tissue plates in triplicate for HepG2-HDGF and HepG2-neo, respectively. The cell colonies measuring > 0.1 mm in diameter were counted after 3 weeks of incubation at 37°C and 5% CO_2 in air, under a microscopic field at x 40 magnifications. The means were based on numbers from triplicate wells for each treatment condition and were analyzed using two-tailed Student's *t* test.

Tumorigenicity in nude mice

Four-week-old male BALB/cA Jcl-nu mice were obtained from Japan Clea (Hamamatsu, Japan). Following trypsinization, HeG2-HDGF and HepG2-Neo cells were harvested (2 x 10^6), resuspended in 200 µl of PBS and inoculated subcutaneously into left and right sides in the dorsal region of nude mouse. Two animals were used in each group. The tumor size was measured with a caliper once or twice per week, and the volumes were estimated according to the following formula: volume = maximal length x (perpendicular length)^2 x 0.5. A histological analysis of tumors which developed in the nude mice was performed after hematoxylin-eosin staining as reported previously [7].

DNA chip analysis

The total RNA was extracted from the cultured HepG2 cells and their xenograft tumor tissues using ISOGEN (Wako, Osaka, Japan) and Poly(A)+RNA was purified from total RNA using an Oligotex-Dt30 mRNA purification kit (Takara Otsu, Shiga, Japan).

The expression of each gene was simultaneously analyzed through the hybridization of the targets which were prepared by using Poly(A)+RNA as template. A DNA chip spotted with 886 cDNAs from identified human genes (IntelliGene™ Human CHIP 1K Set I, version 1.0) was acquired from Takara Shuzo, (Kyoto, Japan). The results were also analyzed by normalizing fluorescence intensities between experiments using a subset of cDNA clones.

Statistical analysis

The results are expressed as the means ± SE. At least three separate experiments were performed for each data point except for the DNA chip analysis. Statistical analyses were done using Student's unpaired *t*-test (two-tailed). Differences were considered to be statistically significant whenever a *P* value was < .05.

RESULTS

The over-expression of HDGF enhances the anchorage-independent growth of HCC cells in soft agar

We investigated whether the increased expression of HDGF stimulated the anchorage-independent growth of HCC cells in a soft agar assay. Three weeks after seeding, HepG2-HDGF cells produced significantly more and bigger colonies than HepG2-neo cells (Figure 1). The numbers of colonies (average of triplicate wells with three randomly selected fields per well) visible in a microscopic field at 40 magnifications for the two cell lines were 3.67±0.37 and 2.36±0.38 for HepG2-HDGF and HepG2-neo cells, respectively. These results suggest that HDGF enhances the anchorage-independent growth of HCC cells.

HDGF over-expression enhances the tumor growth of HCC cells *in vivo*

As shown in Figure 2, the HepG2-HDGF cells generated tumors at 4 weeks after injection, and these tumors increased in size over time. The tumor volume in the mice were 1,666±238 mm^3 and 442±26 mm^3 at 9 weeks after the inoculation of HepG2-HDGF and HepG2-neo cells, respectively ($P<0.01$). The tumors formed by HepG2-HDGF cells were macroscopically bigger and more reddish than those of HepG2-neo

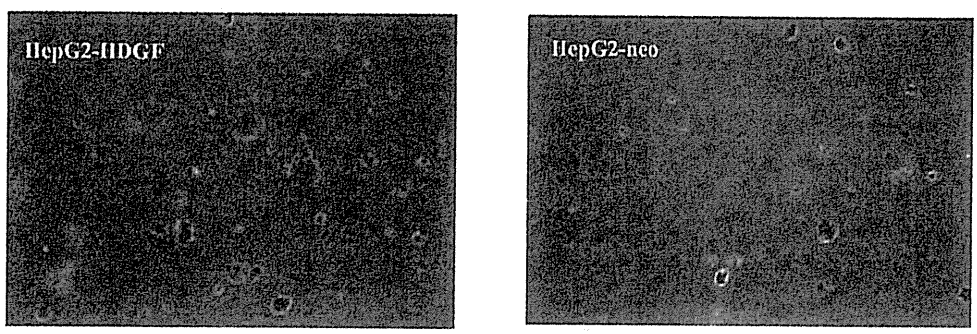

Figure 1. Effect of the HDGF over-expression on HCC cells in anchorage-independent growth. HDGF over-expressing HepG2 (HepG2-HDGF) cells produce larger colonies than mock HepG2 (HepG2-neo) cells in a soft agar assay described in Methods. The representative photos of colonies formed by HepG2-HDGF or HepG2-neo cells after 21-day culture were shown (x 40 magnifications).

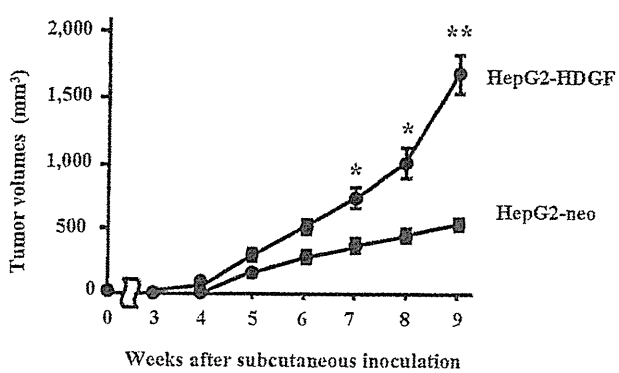

Figure 2. Tumor growth curves of HDGF over-expressing HepG2 cells in nude mice. The tumor volumes of HepG2-HDGF cells or HepG2-neo cells are shown after inoculation in nude mice. Data are shown as the mean ±SE of three independent experiments (n=3). *: $P<0.05$, and **: $P<0.01$, HepG2-HDGF vs. HepG2-neo.

cells (Figure 3a). Moreover, a microscopic examination showed abundant capillary vessel formation (Figure 3b). The expressions of the myc-tagged-HDGF protein in nude mice were confirmed by a Western blot analysis with rabbit polyclonal anti-C terminus of HDGF antibody (Figure 3c). These results suggest that an over-expression of HDGF stimulates the xenograft tumor growth rapidly in nude mice through prominent neovascularization as well as by stimulating the proliferation of cancer cells *in vivo*.

HDGF-regulated genes evaluated by a DNA chip analysis

We performed DNA chip analysis for both cultured cells and tumors generated in nude mice to investigate the up- and down-regulated genes by HDGF over-expression. DNA chip analysis revealed the genes which were differently expressed in HepG2-HDGF and HepG2-neo *in vitro* and *in vivo*. The top 10 genes up-regulated simultaneously both *in vitro* and *in vivo* by HDGF are shown in Table 1. Chitinase 3-like-2 and urokinase-type plasminogen activator (u-PA) were up-regulated more than 10 fold. Coagulation factor II receptor (F2R), matrix metalloproteinase 1 (MMP-1), platelet-derived growth factor alpha (PDGF-A), ankyrin 1, Ser-Thr protein kinase and A kinase anchor protein were up-regulated more than 2 fold. When we focus on the growth factors, growth factor-related proteins and their receptors, seven genes including PDGF-A were significantly up-regulated in the tumors generated from HepG2-HDGF cells in nude mice (Table 2). However, theses factors and receptors are induced more prominently *in vivo* than *in vitro* except for PDGF-A. Especially, Tyrosine kinase with Ig and EGF-like domains (Tie-1), schwannoma-derived growth factor (amphiregulin), AXL receptor tyrosine kinase are up-regulated more than 10 fold *in vivo*. On the other hand, the only gene that was down-regulated more than 2 fold by HDGF over-expression was connective tissue growth factor (CTGF), which decreased to 0.44 and 0.41 fold in cultured cells and xenograft tumors, respectively.

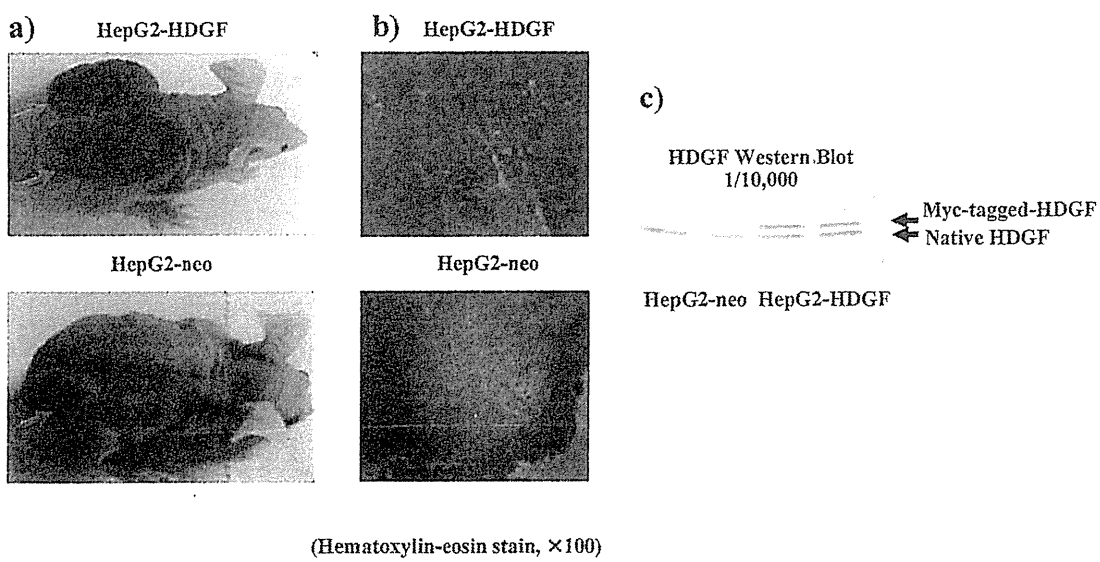

Figure 3. Tumors developed by the inoculation of HepG2-HDGF in nude mice.
a) The macroscopic appearance of tumors which developed in nude mice. Photographs show tumors that developed in the nude mice at 9 weeks after the subcutaneous inoculation of either HepG2-HDGF or HepG2-neo cells, respectively. b) Microscopic photographs of tumors which formed by HepG2-HDGF or HepG2-neo. Histological findings by hematoxylin-eosin staining show the tumors derived from HepG2-HDGF cells more rich in vasculature than HepG2-neo cells. c) The *in vivo* expression of myc-tagged-HDGF protein in each clone is shown in a Western blot analysis with rabbit polyclonal anti-C terminus HDGF antibody.

Table 1. The top 10 genes that were up-regulated in HepG2 cells by HDGF over-expression both *in vitro* and *in vivo*.

Genes	Rates of induction	
	Cell line	Nude mouse
Chitinase 3-like 2	17.99	9.42
Plasminogen activator, urokinase (u-PA)	17.97	4.77
Coagulation factor II receptor (F2R)	3.01	2.20
Matrix metalloproteinase 1 (MMP-1)	2.94	2.55
Platelet-derived growth factor alpha (PDGF-A)	2.59	3.85
Ankyrin 1	2.50	3.11
Ser-Thr protein kinase	2.30	3.51
A kinase (PPKA) anchor protein	2.24	2.06
Dystrophin	1.91	3.12
G protein-coupled receptor 105	1.89	3.51

Table 2. Top 7 genes of growth factors and their receptors that were up-regulated in tumors generated from HDGF over-expressing HepG2 cells in nude mice.

Genes	Rates of induction	
	Nude mouse	Cell line
Tyrosine kinase with Ig and EGF-like domains (Tie-1)	21.78	IC
Schwannoma-derived growth factor (Amphiregulin)	16.57	0.28
AXL receptor tyrosine kinase	14.05	IC
Bone morphogenetic protein 6 (BMP6)	6.43	IC
Leukemia inhibitory factor (LIF)	5.46	0.49
Epithelial cell receptor protein tyrosine kinase (EphA2)	4.82	0.31
Platelet-derived growth factor alpha polypeptide (PDGF-A)	3.85	2.59

IC: Incomparable due to no detectable signal in control or/and samples.

DISCUSSION

The established HepG2 clones which stably over-express HDGF stimulate not only the anchorage-independent colony formation in a soft agar, but also generate tumors and enhance the tumor growth in nude mice. Another study using gastric adenocarcinoma cells showed similar results, namely that HDGF transfection also promoted anchorage-independent growth in soft agar [17]. On the other hand, the down-regulated HDGF expression in non-small cell lung cancer (NSCLC) cells reduced the colony formation in soft agar and inhibited the invasive potential across the Matrigel membrane [9]. As reported previously, NIH3T3-HDGF cells generated tumors in nude mice, but the mock and wild NIH3T3 cells did not. The HDGF over-expression in NIH3T3 cells induced tumorigenesis *in vivo* through both a direct angiogenic activity and the induction of vascular endothelial growth factor (VEGF), but these HDGF-over-expressing cells could not form colonies of any significant size in soft agar [7]. NIH3T3 cells are a non-transformed cell line, derived from mouse fibroblasts. Conversely, HepG2 cell is a transformed cell line derived from hepatoblastoma cells as well as NSCLC cell line, A549 and gastric cancer cell

line, AGS [9, 17]. HDGF alone does not have the ability to form colonies of significant size in a soft agar assay, but it can generate tumors in nude mice. Therefore, other factor(s) are required to achieve *in vitro* anchorage-independent cell growth in soft agar, in addition to HDGF over-expression. In cancer derived transformed cells, these factors have already been expressed and then HDGF produced a large number of colonies of significant size of cancer cells in soft agar. *In vivo*, both HDGF over-expressing NIH3T3 cells and HepG2 cells generated tumors in nude mice. Therefore, HDGF may be responsible for both tumor formation and growth *in vivo*.

Down-regulated HDGF in NSCLC cells inhibits the tumor growth and markedly reduces blood vessel formation in nude mice [9]. In the present study, HDGF over-expression was observed to promote tumor growth, while also stimulating vessel formation in nude mice. HDGF can directly stimulate the endothelial cell proliferation and induce VEGF, thus resulting in prominent angiogenesis *in vivo* [7]. According to the DNA chip results both *in vitro* and *in vivo*, another vascular growth factor, PDGF-A is up-regulated by an over-expression of HDGF. PDGF-A is a growth factor which is closely related to the proliferation of HCC cells [22]. Therefore, these findings suggest that HDGF promotes the tumor growth *in vivo* through the enhanced angiogenesis by the induction of these angiogenic factors in addition to its direct angiogenic activity.

Some genes related to the biologically aggressive characteristics of tumors including invasion and metastasis are up-regulated by HDGF over-expression both *in vitro* and *in vivo* according to a DNA chip analysis. The up-regulation of chitinase 3-like-2 is associated with a poor survival in glioblastoma, and an over-expression of ankyrin has been reported to contribute to hepatocarcinogenesis by destabilizing the retinoblastoma gene [23, 24]. The down regulation of u-PA by small interfering RNA has been reported to suppress the invasion and migration of human HCC cells [25]. Another up-regulated gene, MMP-1 is also closely involved in tumor invasion. MMP-1 is expressed in early HCC, and conversely the reduced activity of MMP-1 by MMP inhibitor potently suppresses the invasion of HCC cells [26, 27]. Therefore, HDGF may display either an invasive or metastatic activity through the induction of these genes.

Furthermore, when we focus on these growth factors, their receptors and signal transduction proteins, some molecules related in tumor biology are up-regulated by an HDGF over-expression in tumors which developed *in vivo*. The Tie-1 expression is up-regulated at 22 fold in tumors derived from HepG2-HDGF cells in comparison to those from HepG2-neo cells *in vivo*, but it is not up-regulated in cells *in vitro*. Tie-1, which is predominantly expressed in blood vessel endothelial cells, is deeply involved in angiogenesis [28]. Tie-1 is reported to be highly expressed in large HCCs and may be a novel independent prognostic marker for gastric cancer [29, 30]. Tie-1 may be involved in the rich vasculature in HepG2-HDGF-derived tumors, after its induction in endothelial cells by the paracrine effect of HDGF. AXL is up-regulated by 14 fold in tumors from HepG2-HDGF cells in comparison to those from HepG2-neo cells. AXL has been reported to be highly expressed in multiple types of cancers including HCC, and it has also been linked to an adverse clinical outcome in patients with cancer [31]. Interestingly, AXL has been demonstrated to be significantly down-regulated by HDGF siRNA treatment in NSCLC-derived tumors in nude mice [9]. These facts suggest that AXL induction by HDGF may thus play an important role as one pathway to display the biological aggressiveness of cancers.

Conversely, only one gene, CTGF is down-regulated by HDGF over-expression in HepG2 cells and their xenograft tumors. CTGF exhibits a variety of biological functions of tumor cells, including cell adhesion, migration and proliferation. An elevated expression of CTGF has been detected in several cancers, and the inhibition of CTGF with a monoclonal antibody suppresses pancreatic tumor growth and metastasis [32]. An increased expression of CTGF was associated with a decreased survival of patients with breast cancer, glioblastoma or esophageal adenocarcinoma [33-35]. In contrast, a high level of CTGF has been reported to be associated with better survival in patients with

esophageal squamous cell carcinoma and chondrosarcoma, and its reduced expression has also been shown to be correlated with the disease stage and decreased survival in lung adenocarcinoma [35-37]. In HCC, CTGF has been reported to be highly expressed, however the relationship between the CTGF levels and the disease-free or overall survivals in patients with HCC has not yet been clarified [38, 39]. The down-regulation of CTGF by HDGF suggests that the reduced expression of CTGF may be related to an advanced disease stage and the malignant potentials in HCC cells. Further studies should thus be conducted to elucidate the role of CTGF on HCC cells.

In conclusion, we confirmed that HDGF over-expression in HCC cell lines promoted the anchorage-independent growth of HCC cells and the xenograft tumor formation, and regulated the expression of the genes which were related to tumor biology. These findings are consistent with the clinical evidence that a higher expression of HDGF in tumors has more aggressive characteristics, including distant metastasis and invasion, and a higher recurrence and poorer survival. Therefore, HDGF promotes tumorigenesis and tumor progression not only through its direct angiogenic activity and cell proliferation stimulating activity but also due to the up-regulation and down-regulation of the genes, that are involved in tumor biology and angiogenesis. Future studies should focus on analyzing the detailed molecular mechanisms of HDGF-induced tumor development and progression, in order to eventually develop a treatment modality to regulate the action of HDGF protein and the molecules related in its signal transduction pathway in order to develop potential therapeutically effective applications.

ABBREVIATIONS

HDGF, hepatoma-derived growth factor; PDGF, platelet-derived growth factor; CTGF, connective tissue growth factor; Tie-1, tyrosine kinase with Ig and EGF-like domains; u-PA, urokinase-type plasminogen activator; MMP-1, matrix metallo-proteinase 1; HCC, hepatocellular carcinoma; NSCLC, non-small cell lung cancer

REFERENCES

1. Nakamura, H., Kambe, H., Egawa, T., Kimura, Y., Ito, H., Hayashi, E., Yamamoto, H., Sato, J., and Kishimoto, S. 1989, Clin. Chim. Acta, 183, 273.
2. Nakamura, H., Izumoto, Y., Kambe, H., Kuroda, T., Mori, T., Kawamura, K., Yamamoto, H., and Kishimoto, T. 1994, J. Biol. Chem., 269, 25143.
3. Oliver, J, A., and Al-Awqati, Q. 1998, J. Clin. Invest., 102, 1208.
4. Everett, A. D., Lobe, D. R., Matsumura, M. E., Nakamura, H., and McNamara, C. A. 2000, J. Clin. Invest., 105, 567.
5. Everett, A. D., Stoops, T., and McNamara, C. A. 2001, J. Biol. Chem., 276, 37564.
6. Kishima, Y., Yamamoto, H., Izumoto, Y., Yoshida, K., Enomoto, H., Yamamoto, M., Kuroda, T., Ito, H., Yoshizaki, K., Nakamura, H. 2002, J. Biol. Chem., 277, 10315.
7. Okuda, Y., Nakamura, H., Yoshida, K., Enomoto, H., Uyama, H., Hirotani, T., Funamoto, M., Ito, H., Everett, A. D., Hada, T., and Kawase, I. 2003, Cancer Sci., 94, 1034.
8. Kishima, Y., Yoshida, K., Enomoto, H., Yamamoto, M., Kuroda, T., Okuda, Y., Uyama, H., and Nakamura, H. 2002, Hepatogastroenterology, 49, 1639.
9. Zhang, J., Ren, H., Yuan, P., Lang, W., Zhang, L., and Mao, L. 2006, Cancer Res., 66, 18.
10. Yoshida, K., Nakamura, H., Okuda, Y., Enomoto, H., Kishima, Y., Uyama, H., Ito, H., Hirasawa, T., Inagaki, S., and Kawase, I. 2003, J. Gastroenterol. Hepatol., 18, 1293.
11. Hu, T. H., Huang, C. C., Liu, L. F., Lin, P. R., Liu, S. Y., Chang, H. W., Changchien, C. S., Lee, C. M., Chuang, J. H., and Tai, M. H. 2003, Cancer, 98, 1444.
12. Yoshida, K., Tomita, Y., Okuda, Y., Yamamoto, S., Enomoto, H., Uyama, H., Ito, H., Hoshida, Y., Aozasa, K., Nagano, H., Sakon, M., Kawase, I., Monden, M., and Nakamura, H. 2006, Ann. Surg. Oncol., 13, 1.
13. Ren, H., Tang, X., Lee, J. J., Feng, L., Everett, A. D., Hong, W. K., Khuri, F. R., and Mao, L. 2004, J. Clin. Oncol., 22, 3230.

14. Iwasaki, T., Nakagawa, K., Nakamura, H., Takada, Y., Matsui, K., and Kawahara, K. 2005, Oncol. Rep., 13, 1075.
15. El-Rifai, W., Frierson, H. F. Jr., Harper, J. C., Powell, S. M., and Knuutila, S. 2001, Int. J. Cancer., 92, 832.
16. Yamamoto, S., Tomita, Y., Hoshida, Y., Takiguchi, S., Fujiwara, Y., Yasuda, T., Doki, Y., Yoshida, K., Aozasa, K., Nakamura, H., and Monden, M. 2006, Clin. Cancer Res., 12, 117.
17. Mao, J., Xu, Z., Fang, Y., Wang, H., Xu, J., Ye, J., Zheng, S., and Zhu, Y. 2008, Cancer Sci., 99, 2120.
18. Everett, A. D., Narron, J. V., Stoops, T., Nakamura, H., and Tucker, A. 2004, Am. J. Physiol. Lung Cell Mol. Physiol., 286, L1194.
19. Yamamoto, S., Tomita, Y., Hoshida, Y., Morii, E., Yasuda, T., Doki, Y., Aozasa, K., Uyama, H., Nakamura, H., and Monden, M. 2007, Ann. Surg. Oncol., 14, 2141.
20. Uyama, H., Tomita, Y., Nakamura, H., Nakamori, S., Zhang, B., Hoshida, Y., Enomoto, H., Okuda, Y., Sakon, M., Aozasa, K., Kawase, I., Hayashi, N., and Monden, M. 2006, Clin. Cancer Res., 12 (20 Pt 1), 6043.
21. Chang, K. C., Tai, M. H., Lin, J. W., Wang, C. C., Huang, C. C., Hung, C. H., Chen, C. H., Lu, S. N., Lee, C. M., Changchien, C. S., and Hu, T. H. 2007, Int. J. Cancer, 121, 1059.
22. Stock, P., Monga, D., Tan, X., Micsenyi, A., Loizos, N., and Monga, S. P. 2007, Mol. Cancer Ther., 6, 1932.
23. Saidi, A., Javerzat, S., Bellahcène, A., De Vos, J., Bello, L., Castronovo, V., Deprez, M., Loiseau, H., Bikfalvi, A., and Hagedorn, M. 2008, Int. J. Cancer, 122, 2187.
24. Higashitsuji, H., Itoh, K., Nagao, T., Dawson, S., Nonoguchi, K., Kido, T., Mayer, R. J., Arii, S., and Fujita, J. 2000, Nat. Med., 6, 96.
25. Salvi, A., Arici, B., De Petro, G., and Barlati, S. 2004, Mol. Cancer Ther., 3, 671.
26. Murakami, K., Sakukawa, R., Ikeda, T., Matsuura, T., Hasumura, S., Nagamori, S., Yamada, Y., and Saiki, I. 1999, Neoplasia., 1, 424.
27. Okazaki, I., Wada, N., Nakano, M., Saito, A., Takasaki, K., Doi, M., Kameyama, K., Otani, Y., Kubochi, K., Niioka, M., Watanabe, T., and Maruyama, K. 1997, Hepatology, 25, 580.
28. Tang, Y., Borgstrom, P., Maynard, J., Koziol, J., Hu, Z., Garen, A., and Deisseroth, A. 2007, Cancer Gene Ther., 14, 346.
29. Dhar, D. K., Naora, H., Yamanoi, A., Ono, T., Kohno, H., Otani, H., and Nagasue, N. 2002, Anticancer Res., 22(1A), 379.
30. Lin, W. C., Li, A. F., Chi, C. W., Chung, W. W., Huang, C. L., Lui, W. Y., Kung, H. J., and Wu, C. W. 1999, Clin. Cancer Res., 5, 1745.
31. Tsou, A. P., Wu, K. M., Tsen, T. Y., Chi, C. W., Chiu, J. H., Lui, W. Y., Hu, C. P., Chang, C., Chou, C. K., and Tsai, S. F. 1998, Genomics, 50, 331.
32. Dornhöfer, N., Spong, S., Bennewith, K., Salim, A., Klaus, S., Kambham, N., Wong, C., Kaper, F., Sutphin, P., Nacamuli, R., Höckel, M., Le, Q., Longaker, M., Yang, G., Koong, A., and Giaccia, A. 2006, Cancer Res., 66, 5816.
33. Xie, D., Nakachi, K., Wang, H., Elashoff, R., and Koeffler, H. P. 2001, Cancer Res., 61, 8917.
34. Xie, D., Yin, D., Wang, H. J., Liu, G. T., Elashoff, R., Black, K., and Koeffler, H. P. 2004, Clin. Cancer Res., 10, 2072.
35. Koliopanos, A., Friess, H., di Mola, F. F., Tang, W. H., Kubulus, D., Brigstock, D., Zimmermann, A., and Büchler, M. W. 2002, World J. Surg., 26, 420.
36. Shakunaga, T., Ozaki, T., Ohara, N., Asaumi, K., Doi, T., Nishida, K., Kawai, A., Nakanishi, T., Takigawa, M., and Inoue, H. 2000, Cancer, 89, 1466.
37. Chang, C. C., Shih, J. Y., Jeng, Y. M., Su, J. L., Lin, B. Z., Chen, S. T., Chau, Y. P., Yang, P. C., and Kuo, M. L. 2004, J. Natl. Cancer Inst., 96, 364.
38. Hirasaki, S., Koide, N., Ujike, K., Shinji, T., and Tsuji, T. 2001, Hepatol. Res., 19, 294.
39. Zeng, Z. J., Yang, L. Y., Ding, X., and Wang, W. 2004, World J. Gastroenterol., 10, 3414.

Hepatology Research

Hepatology Research 2010; **40**: 823–831 doi: 10.1111/j.1872-034X.2010.00670.x

Original Article

Crucial role of impaired Kupffer cell phagocytosis on the decreased Sonazoid-enhanced echogenicity in a liver of a nonalchoholic steatohepatitis rat model

Shohei Yoshikawa,[1] Hiroko Iijima,[1] Masaki Saito,[1] Hironori Tanaka,[1] Hiroyasu Imanishi,[1] Naoki Yoshimoto,[2] Tomohiro Yoshimoto,[3] Shizue Futatsugi-Yumikura,[4] Kenji Nakanishi,[4] Tohru Tsujimura,[5] Takashi Nishigami,[5] Atsushi Kudo,[6] Shigeki Arii[6] and Shuhei Nishiguchi[1]

[1]*Division of Hepatobiliary and Pancreatic Diseases, Department of Internal Medicine, Hyogo College of Medicine,* [2]*Ultrasound Imaging Center, Hyogo College of Medicine,* [3]*Laboratory of Allergic Diseases, Institute for Advanced Medical Sciences, Hyogo College of Medicine,* [4]*Department of Immunology and Medical Zoology, Hyogo College of Medicine,* [5]*Department of Pathology, Hyogo College of Medicine, and* [6]*Department of Hepatobiliary Pancreatic Surgery, Tokyo Medical and Dental University, Tokyo, Japan*

Aims: To evaluate the dynamics of Kupffer cell (KC) phagocytosis by performing both *in vivo* and *in vitro* studies using Sonazoid (GE Healthcare, Oslo) in a rat nonalcoholic steatohepatitis (NASH) model.

Methods: Contrast enhanced ultrasonography (CEUS) was performed on a rat NASH model induced by a methionine choline deficient diet (MCDD) and control rats, and Sonazoid was used to measure the signal intensity in the liver parenchyma. The uptake of Sonazoid by the KCs was observed by intravital microscopy. Their phagocytic capability was evaluated *in vitro* using isolated and cultured KCs. The uptake of fluorescein isothiocyanate (FITC)-labeled latex beads was observed and quantitatively analyzed by flow cytometry.

Results: In the MCDD group, liver parenchymal enhancement was reduced 20 min after the Sonazoid injection. Microscopic observation of the isolated and cultured KCs revealed that the number of phagocytosed Sonazoid microbubbles was significantly decreased. Confocal laser scanning microscopic (CLSM) observation showed a decrease in the uptake of the latex beads. A decreased phagocytic capacity in the MCDD group was suggested by the quantitative analysis using flow cytometry, as well as by intravital microscopy.

Conclusions: CEUS with Sonazoid is a powerful evaluation tool to diagnose NASH from an early stage of the disease.

Key words: Kupffer cells, nonalcoholic steatohepatitis, phagocytosis, Sonazoid, ultrasound contrast agents.

INTRODUCTION

NONALCOHOLIC FATTY LIVER disease (NAFLD) has been increasing as the incidence of obesity and metabolic syndrome has been rising. Nonalcoholic steatohepatitis (NASH) draws particular attention due to the risk of progression to cirrhosis and hepatocellular carcinoma.[1–3] Liver biopsy has been considered to be the only way to definitively diagnose NASH[4,5] because diagnosis using imaging modalities is believed to be impossible.[6] In a recent study, magnetic resonance imaging was used for the quantification of the liver fat content and the evaluation of hepatic fibrosis, but it was still inadequate to replace liver biopsy.[7] Liver biopsy is not necessarily recommended for all NAFLD patients because of the risks of the procedure.

We have previously reported the usefulness of contrast enhancement ultrasound (CEUS) in the diagnosis of NASH with a contrast agent, Levovist, which is phagocytosed by the Kupffer cells (KC) in the liver.[8,9] In the liver parenchyma of NASH patients, the accumulation of Levovist microbubbles decreased remarkably 5 min after Levovist injection (especially by 20 min).

Correspondence: Dr Hiroko Iijima, Division of Hepatobiliary and Pancreatic Diseases, Department of Internal Medicine, Hyogo College of Medicine, 1-1 Mukogawa-cho, Nishinomiya, Hyogo 663-8501, Japan. Email: hiroko-i@hyo-med.ac.jp
Received 15 January 2009; revision 17 February 2010; accepted 19 January 2010.

Tsujimoto *et al.* demonstrated reduced contrast effect and phagocytic activity *in vitro* in a rat model prepared by a choline-deficient l-amino acid-defined (CDAA) diet.[10] However, they did not prove it *in vivo* in a rat model that the decreased parenchymal enhancement with Levovist was attributed to phagocytosis by KCs. Sonazoid (GE Healthcare, Oslo) has also been proven to be phagocytosed by KCs.[11,12] We performed CEUS using Sonazoid on a rat NASH model prepared by a methionine choline deficient diet (MCDD)[13] to evaluate the parenchymal enhancement. The phagocytosis of Sonazoid by phagocytic cells was observed *in vivo* in real time by intravital microscopy. To evaluate and prove Sonazoid phagocytosis *in vitro*, isolated and cultured KCs were observed and compared between the MCDD and control groups. Moreover, to evaluate the phagocytic capacity of KCs, the uptake of fluorescein isothiocyanate (FITC)-labeled latex beads was observed and a quantitative analysis was performed using flow cytometry.

METHODS

Animals

THIS STUDY PROTOCOL was approved by the Animal care committee of the Hyogo College of Medicine, and was performed in conformity with their institutional guidelines.

Male Wistar rats (190–200 g; SLC Japan, Tokyo), were housed in the animal facility of the Hyogo College of Medicine and kept at a controlled temperature of 23 ± 1~2°C under 12 h light/12 h dark cycles. Animals for the NASH model were given free access to tap water and MCDD (Oriental Yeast, Tokyo). Animals in the control group had free access to tap water and a normal laboratory diet (MF diet; Oriental Yeast). Animals on the 2nd, 4th and 8th weeks of the diet were used. For observation by intravital microscopy, 25% urethane (Wako Pure Chemical Industries, Osaka) subcutaneous anesthesia was used; and for other observations, isoflurane (Takeda Pharmaceutical, Tokyo) inhalation anesthesia was used.

Histological examination

The liver tissues were fixed in 10% formalin, and then stained with hematoxylin and eosin or Azan. Then, the degree of steatosis, inflammation and fibrosis were assessed from the tissues using the Brunt's histological grading and scoring system.

Preparation of contrast agents and latex beads

The contrast agent Sonazoid and 2.6% FITC-labeled latex beads (Polyscience, Warrington, PA) with diameters of 1 μm and 2 μm, were used. They were diluted with distilled water to 1×10^9 microbubbles/mL and 1×10^9 beads/mL, respectively.

Contrast enhanced ultrasound using Sonazoid

Sonazoid at 0.015 μL (approximately 1.5×10^4 microbubbles)/100g body was injected into the caudal vein after being diluted with distilled water to a total volume of 500 μL.

CEUS was performed by a Toshiba Aplio (Toshiba Medical Systems, Tokyo) with a 7.5 MHz linear transducer. Following conventional B-mode imaging, images were obtained in Advanced Dynamic Flow (ADF) mode with a high mechanical index (MI) of 1.0 to cause destructions of the Sonazoid bubbles. The images were obtained at a focus depth of 3 cm from the body surface at a frame rate of 10 frames/second.

Scanning was performed in various planes of the liver at 20 and 50 min after the Sonazoid injection. This scanning time was based on evidence that the Kupffer phase started at approximately 20 min after the Sonazoid injection when the washout of Sonazoid from the hepatic vein was observed in a healthy volunteer.[14] On the 2nd, 4th, and 8th weeks of the diet, CEUS was performed on four animals from each group to see if any differences in parenchymal enhancement could be detected depending on the duration of the diet. CEUS using ADF was performed at 20 min after the Sonazoid injection to measure the parenchymal intensity within the region of interest (ROI), which was randomly set in the depth within the focus area. The average signal intensity in the liver parenchyma was then calculated after it was converted to sound pressure using the antilog calculation. Scanned images were recorded separately as ADF signals and gray scale signals.

Intravital microscopic observation of phagocytosis by Kupffer cells

Animals in both groups were opened under anesthesia to expose their livers, and were placed in a prone position on a 3 cm diameter transplant platform. A 23 gauge indwelling cannula was inserted into the caudal vein, and 500 μL of 150 μL/100 g Sonazoid diluted with distilled water was administered.

Preparation and phagocytosis of Kupffer cells – *in vitro* study

KCs were isolated from animals in both groups with the previously published procedure: After anesthetizing the animals by isofluran inhalation, the portal vein was cannulated with a 20-gauge needle and the inferior vena cava was opened and a perfusion circuit was created.

Briefly, liver non-parenchymal cells were isolated by the pronase-collagenase method as previously described,[15] and eluted fractions were collected using a Beckman J6-MC centrifuge (Beckman Coulter, Fullerton, CA). The cells were washed, and re-suspended in Roswell Park Memorial Institute (RPMI) 1640 supplemented with 10% fetal bovine serum containing 2-ME (50 μM), L-glutamine (2 mM), penicillin (100 U/mL) and streptomycin (100 μg/mL), plated onto plastic dishes 3.5 cm in diameter, and incubated for 24 h. The plastic adherent cells (1×10^6/mL) were then incubated with 3×10^5 Microbubble/ml Sonazoid for 30 min. After washing the plates with culture medium, the uptake of Sonazoid by the isolated KCs was observed by inverted microscopy (TE300-HM-2; Nikon, Tokyo) in a micro-incubator at 37°C in 5% CO_2. The microscopic images were recorded by image analyzing software (Aquacosmos; Hamamatsu Photonics, Shizuoka). The Sonazoid microbubbles phagocytosed by the KCs were then counted.

Observation of phagocytosis by Kupffer cells – *in vivo* study

Confocal laser scanning microscopy (CLSM)

Latex beads (diameter: 2 μm, concentration: 1×10^8/kg) were administered through the caudal vein of animals from both groups. At 60 min after injection, the animals were sacrificed by anesthesia overdose to prepare frozen sections of the liver. The frozen sections were observed by CLSM (LSM510; Carl Zeiss, Jena).

Flow cytometric quantitative analysis of phagocytic capacity of Kupffer cells

Prior to the experiment, we determined the gating area of KCs fraction using purified KCs according to their forward scatter (FSC) and side scatter (SSC) on a flow cytometer. Once the gated area for KCs was determined, it was used for the rest of the experiments. Aliquots of 1×10^8/kg of FITC-labeled latex beads (diameters: 1 μm and 2 μm) were injected in both groups. At 1 h after injection, KCs isolated by the above-mentioned procedure were cultured for 24 h in an incubator at 37°C in 5% CO_2 to purify the KC fraction and reduce the contaminated cells. Following several washes with phosphate buffered saline (PBS), KCs adhered to the bottom of the dishes were detached with 0.25% Trypsin ethylenediaminetetraacetic acid (EDTA; Invitrogen, Tokyo). They were then centrifuged, and RPMI was added to the sediment to make a total volume of 1 mL in a culture tube. KCs in the tube were then analyzed by flow cytometry. The equipment used was a FACScan (BD Bioscience, San Jose, CA).

Statistics

The statistical significance of the signal intensity change in both groups was evaluated using a repeated measures analysis of variance (ANOVA) test. The Kruskal–Wallis test and Scheffe's *F*-test were performed for a comparison of the phagocytic capacity of isolated and cultured KCs between both groups. All data were analyzed by a statistical software package (SPSS, Chicago, IL).

RESULTS

Changes in liver histology

THE HISTOLOGICAL CHANGES were found as follows: the MCDD-2wk group revealed inflammation and steatosis, but no fibrosis. The MCDD-4wk group showed inflammation, steatosis and slight fibrosis, which was equivalent to grade 2/stage 2 of Blunt's grading/staging system. Inflammation and steatosis were found in the MCDD-8wk group, and their fibrosis was more severe than the one in the MCDD-4wk group, and was corresponding to Blunt's grade 2 /stage 3.

Sonazoid CEUS examination

The signal intensity decreased after Sonazoid injection in the MCDD group as compared to the control group. The quantification of the signal intensity at 20 min after injection is shown in Figure 1. The parenchymal intensity in the control group was −5.0 and −5.5 at 20 and 50 min after Sonazoid injection, respectively, but was −13.0 and −13.3 in the MCDD-4wk group, respectively. In the control group, the intensity decreased slightly to −3.5dB, −4.8dB and −5.5dB on the 2nd, 4th and 8th weeks of administration, respectively. In contrast, in the MCDD group, the intensity decreased according to the duration of the diet administration as to −11.5dB, −13.0dB and −20.5dB on the 2nd, 4th and 8th weeks, respectively; this was a significant difference between the groups ($P < 0.05$) (Figs 1,2).

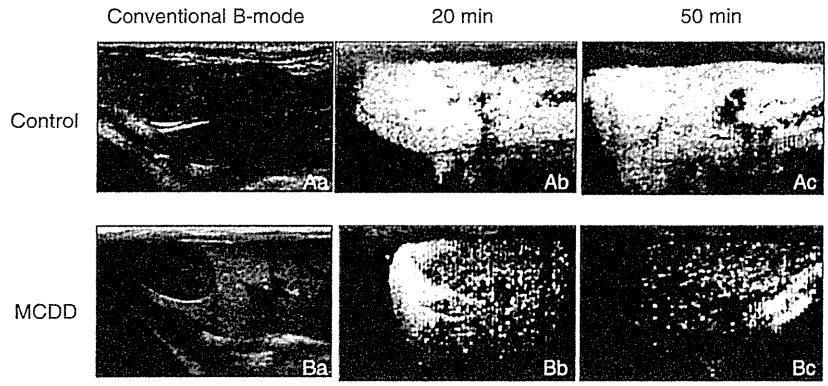

Figure 1 Abdominal US B-mode images (Aa, Ba) and Sonazoid CEUS images (Ab, Ac, Bb, Bc) of control rats (Aa-c) and MCDD-4wk fed rats (Ba-c). The hepato-renal echo contrast was greater in the MCDD rat group as compared with the control group. The livers in the control rats were clearly enhanced until 50 min after injection. In contrast, the enhancement of the liver decreased in the MCDD rats at both 20 and 50 min after injection.

Time course change of Sonazoid phagocytosis observed by intravital microscopy

Five animals from each group were compared. Particles appeared on the sinusoidal wall were observed almost simultaneously at Sonazoid administration, and then the uptake of Sonazoid by phagocytic cells on the sinusoidal wall was recorded using a fixed camera in the view area of the portal vein before Sonazoid injection until 30 min after injection (Fig. 3). The time course was observed by intravital microscopy for 30 min after the Sonazoid injection, and showed that the number of Sonazoid microbubbles phagocytosed by the KCs kept increasing in the control group. However, in the MCDD group, only several Sonazoid microbubbles were phagocytosed by the KCs (Fig. 4).

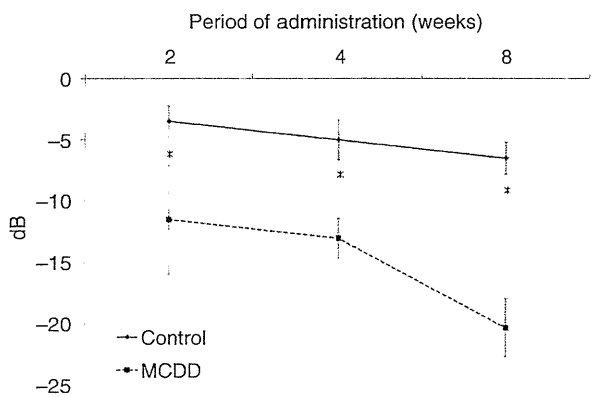

Figure 2 Liver parenchymal intensity (dB) of Sonazoid CEUS on control and MCDD rats at 2 weeks, 4 weeks and 8 weeks of diet administration. The vertical axis is the signal intensity (dB) and the horizontal axis is the duration of diet administration. The parenchymal intensity in the MCDD group showed a decrease as compared with the control group at −11.5dB, −13dB and −20.5dB at the 2nd, 4th, and 8th weeks after administration, respectively ($P < 0.05$).

Phagocytosis of FITC-labeled latex beads by Kupffer cells – *in vivo*

CLSM observations

The number of FITC-labeled latex beads phagocytosed by the KCs and stained as fluorescent green was compared between the two groups. The number of fluorescent-green phagocytosed latex beads in the MCDD group decreased in comparison with the control group, and this suggested decreased phagocytic capacity of the Kupffer cells in the MCDD group (Fig. 5).

Phagocytosis of isolated Kupffer cells – *in vitro*

The inverted microscopic observation of isolated and cultured KCs with Sonazoid is shown in Figure 6. Significant differences were found between the control group and each week of the MCDD groups, and also between the MCDD-2wk and MCDD-8wk groups and between the MCDD-4wk and MCDD-8wk groups ($P < 0.01$) (Fig. 6).

Phagocytosis capability by flow cytometric analysis

Flow cytometric analysis was performed to quantify the phagocytic capacity of isolated and cultured KCs, which were treated with fluorescent latex beads. The phagocytosis rate in the control group was 88%, and many latex beads were ingested. In contrast, the rate was 61% in the MCDD-2wk (B), 37% in the MCDD-4wk (C) and 27% in the MCDD-8wk (D) groups, where the phagocytic capacity had decreased in proportion to the duration

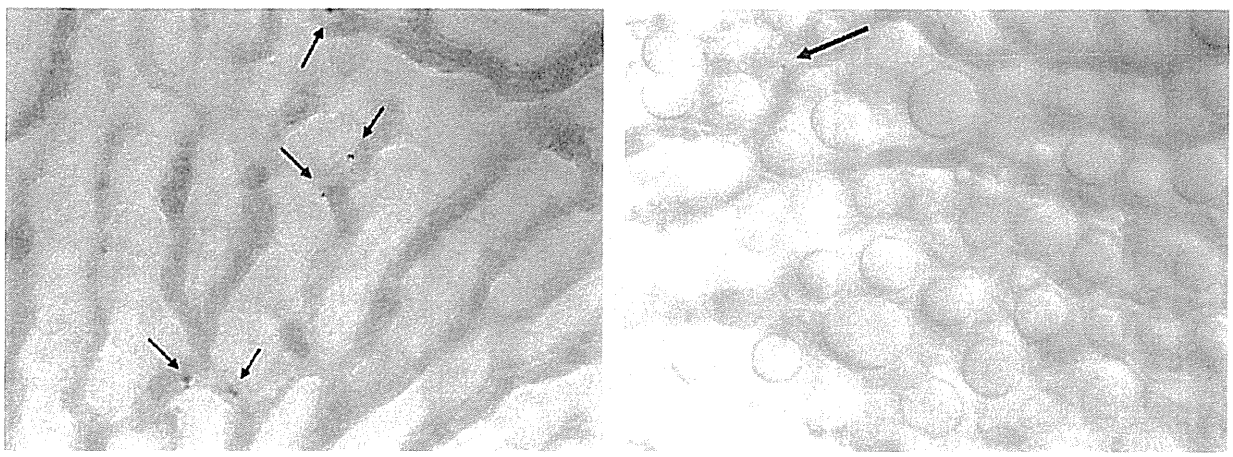

Figure 3 Intravital microscopic observation at 30 min after Sonazoid injection. A number of Sonazoid were phagocytosed by phagocytic cells in the control group; whereas a couple of them were phagocytosed in the MCDD-2wk group.

of the MCDD administration. The phagocytosis index (expressed by the number of KCs which phagocytosed beads/the total number of KCs) in the MCDD group was also lower than in the control groups at every duration of the MCDD administration (Fig. 7). This finding revealed that the phagocytic capacity started to decrease at the early stages of the disease, and kept on decreasing week by week.

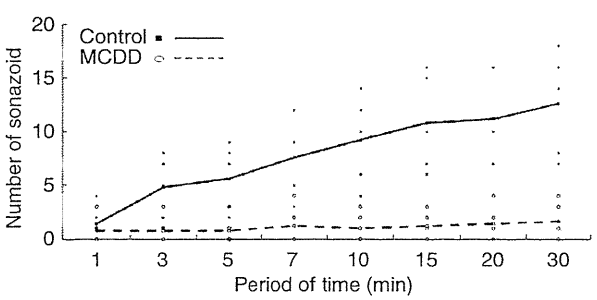

Figure 4 Time-course change in the phagocytosis of Sonazoid. The number of Sonazoid microbubbles phagocytosed by the KCs was plotted at 1, 3, 5, 7, 10, 15, 20 and 30 min after the Sonazoid injection. The control group is shown with a solid line and the MCDD-2wk group is shown with a broken line. Significant difference was seen in the two groups ($P < 0.001$). In the control group, the phagocytosis of Sonazoid increased up to 30 min after Sonazoid injection. In the MCDD-2wk group, only a couple of Sonazoid microbubbles were phagocytosed over a couple min after the injection.

DISCUSSION

NASH HAS BEEN increasing worldwide, and is the most common form of non-alcoholic/non-viral liver disease in the United States and European countries.[16] NAFLD was once considered a benign, reversible condition, and therefore was often left untreated. However, since NASH was introduced by Ludwig, a strong risk of this disease progressing to cirrhosis and hepatocellular carcinoma has been identified.[1–3] In the United States, an estimate shows about 30% of the population has NAFLD, and about 10% of these NAFLD patients has NASH.[17] In countries other than the United States, many people are believed to be developing NASH as their diets become Westernized.[18]

Ultrasonography is used for various organs as a non-invasive diagnostic modality. Ultrasound diagnosis with an intravenous contrast agent is also widely used, and has become indispensable especially in diagnosing the liver diseases.[19,20] The sonographic features of NAFLD including NASH are a high-level echo, a bright liver, vascular blurring, deep attenuation and hepatorenal contrast.[21–24] Abdominal computerized tomography (CT), which provides a more objective assessment, diagnoses NAFLD when the liver to spleen ratio (L/S ratio) is less than 0.9.[25] Thus, the diagnosis of NAFLD could be easily made by these imaging modalities, although distinguishing NASH from NAFLD is considered to be difficult by means of only imaging modalities and blood tests or an invasive liver biopsy is

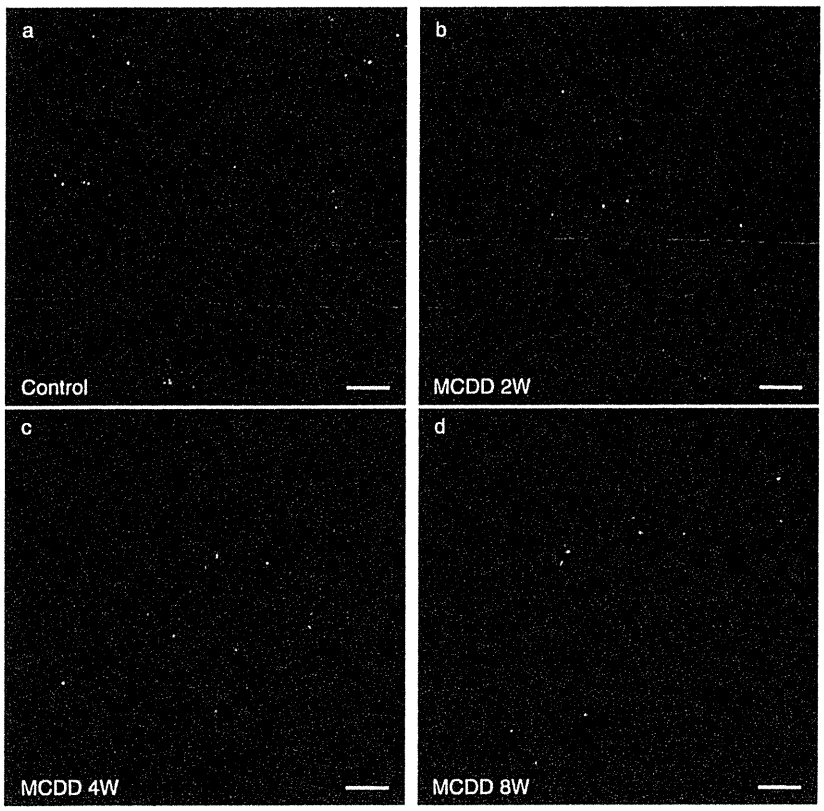

Figure 5 The animals were sacrificed at 60 min after fluorescent latex beads injection and were observed by CLSM. Many latex beads were observed in the control rats (shown in A) as compared with the MCDD rats (in B-D). The fluorescent agent of the latex beads is recognized as green.

required.[4–6] Given the prevalence of NAFLD patients, which has been reported to be as high as 30% of adults who get a medical checkup,[4–6] establishing non-invasive and reliable methods for diagnosing NASH is urgently needed. In the past, we have reported the usefulness of CEUS diagnosis using Levovist to distinguish NASH from NAFLD[9] because it is not realistic to perform liver biopsies for so many NAFLD patients. The diagnosis is made possible by the fact that the liver parenchymal enhancement significantly decreases in NASH patients at 20 min after Levovist injection during the delayed parenchymal phase. One suspected reason for this is the decreased phagocytic capacity of KCs in NASH.[9] Levovist was proven to be phagocytosed by KCs.[11] Furthermore, a study using latex beads on a rat NASH model prepared by a CDAA diet also showed reduced KC phagocytic function, with no changes in the KC numbers, in which the decreased parenchymal contrast effect was possibly attributed to a decrease in the phagocytic capability of KCs, although it did not prove that Levovist itself was phagocytosed by KCs.[10] Moreover, a recent study reported that the engulfment of erythrocytes by KCs was observed by electron microscopy in a rat NASH model induced by a high-fat diet.[26]

Sonazoid is a microbubble with a diameter of 2–4 μm, and contains perfulbutane gas. It has a phospholipid shell which is negatively charged on its surface, and is known to be phagocytosed by liver macrophages, the KCs.[27,28] A report showed that 99% of Sonazoid and 47% of Levovist microbubbles were phagocytosed by isolated and cultured rat KCs;[11] In other words, Sonazoid is expected to be more readily phagocytosed than Levovist. In the present study, the time-course change of KC phagocytosis was investigated by performing CEUS on both MCDD and control rats using Sonazoid by intravital microscopy, and by analyzing isolated and cultured KCs. Sonazoid CEUS performed on a rat NASH model at 20 and 50 min after Sonazoid injection showed a significant decrease in enhancement at 50 min (Fig. 1). Using intravital microscopic observation, the Sonazoid continued to be phagocytosed in the control group, whereas in the MCDD group, the number of phagocytosed Sonazoid

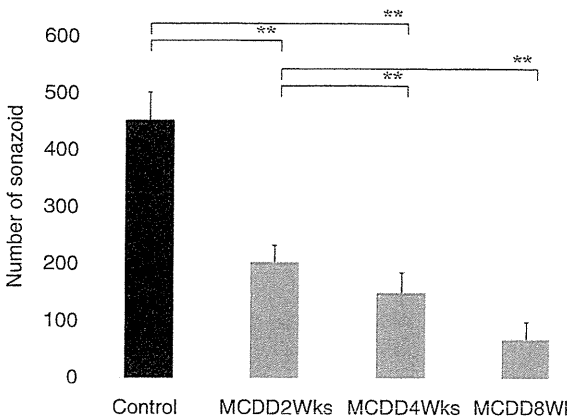

Figure 6 The number of Sonazoid microbubbles phagocytosed by isolated KCs in the control group and the MCDD-2wk, 4wk and 8wk groups were observed by inverted microscopy. After Sonazoid was added, the isolated KCs were cultured before observation. The number of Sonazoid microbubbles phagocytosed by 10 KCs in the control group was 450.5 ± 48.5, whereas 204.1 ± 28.7, 150.9 ± 34.2, and 69.7 ± 29.1 microbubbles were phagocytosed in the MCDD-2wk, 4wk and 8wk groups, respectively (mean ± standard deviation). Significant differences were found between the control group and each week of the MCDD groups, and also between the MCDD-2wk and MCDD-8wk groups and between the MCDD-4wk and MCDD-8wk groups ($P < 0.01$).

microbubbles by phagocytic cells was few after injection. Considering that most of phagocytic cells on sinusoidal wall are KCs, it is reasonable to think contrast agent is phagocytosed by KCs in hepatic sinusoids. Time-course observation also showed the number of phagocytosed microbubbles by phagocytic cells did not increase in the MCDD group (Fig. 4). This finding suggests that the phagocytic capability of KCs may start to decrease during the early stage of NASH, and that could enable the diagnosis of NASH at an early stage of fibrosis. To demonstrate these findings using isolated and cultured KCs, the number of phagocytosed Sonazoid microbubbles decreased in the MCDD rats (Fig. 6). In addition, the number of phagocytosed Sonazoid or latex beads tended to decrease in proportion to the duration of the MCDD administration (Fig. 5). In NASH patients, fibrosis is often detected at a late stage of the disease, because NASH is usually monitored as NAFLD. However, by using Sonazoid CEUS, the diagnosis of NASH could be possible at an early stage, and this represents a groundbreaking development in NASH treatment.

Our study also suggested the clinical usefulness of Sonazoid CEUS in the diagnosis of NASH by demonstrating that: (i) parenchymal enhancement was decreased in the delayed parenchymal phase; and (ii) the phagocytic capacity of Kupffer cells was lowered as the duration of MCDD administration increased. Considering that Sonazoid is specifically phagocytosed by Kupffer cells, the quantification of phagocytic capacity should also be possible.

Some studies have reported the narrowed sinusoids seen in steatosis and steahohepatitis disturb the hepatic microcirculation.[29–31] In particular, the sinusoidal space of a NAFLD animal model was reduced by up to 50 % of the size of healthy control animals.[31] In order to preclude the possibility that the lowered liver parenchymal enhancement was caused by a circulatory disturbance of the contrast agent, latex beads with a diameter of 1 μm, which is smaller than the diameter of Sonazoid (2 μm), were used in the present *in vivo* study, since the width of a normal sinusoid is approximately 5 μm. We performed CEUS with Levovist (4 mL/body) at one minute after Levovist intravenous injection in the early vascular phase to see if decreased parenchymal enhancement was associated with the narrowed sinusoids. Additionally, the parenchymal enhancement of fatty liver patients, NASH patients and healthy volunteers at 1 min after Levovist injection showed a similar intensity in the liver parenchyma in the early vascular phase (Fig. 8). These results demonstrated that the decreased enhancement of liver parenchyma was not due to the narrowed sinusoids or circulatory disturbances.

As shown above, our results suggested decreased Sonazoid-enhanced echogenicity was mainly due to impaired KC phagocytosis, although narrowed sinusoids could be present in MCDD rats due to fatty liver. Sonazoid CEUS could become a useful tool to distinguish NASH patients from many NAFLD patients.

ACKNOWLEDGEMENTS

THIS STUDY WAS supported by a Grant-in-Aid for Scientific Research from the Ministry of Education, Culture, Sports, Science and Technology of Japan, nos. 19500428 and 21300194 and a Grant-in-Aid for Researchers, Hyogo College of Medicine.

We thank all of our colleagues in the Division of Hepatobiliary and Pancreatic Medicine, Ms Sayaka Fujii and Ms Mayumi Yamada, for providing support for our experiments, and the technicians in the Ultrasound Imaging Center.

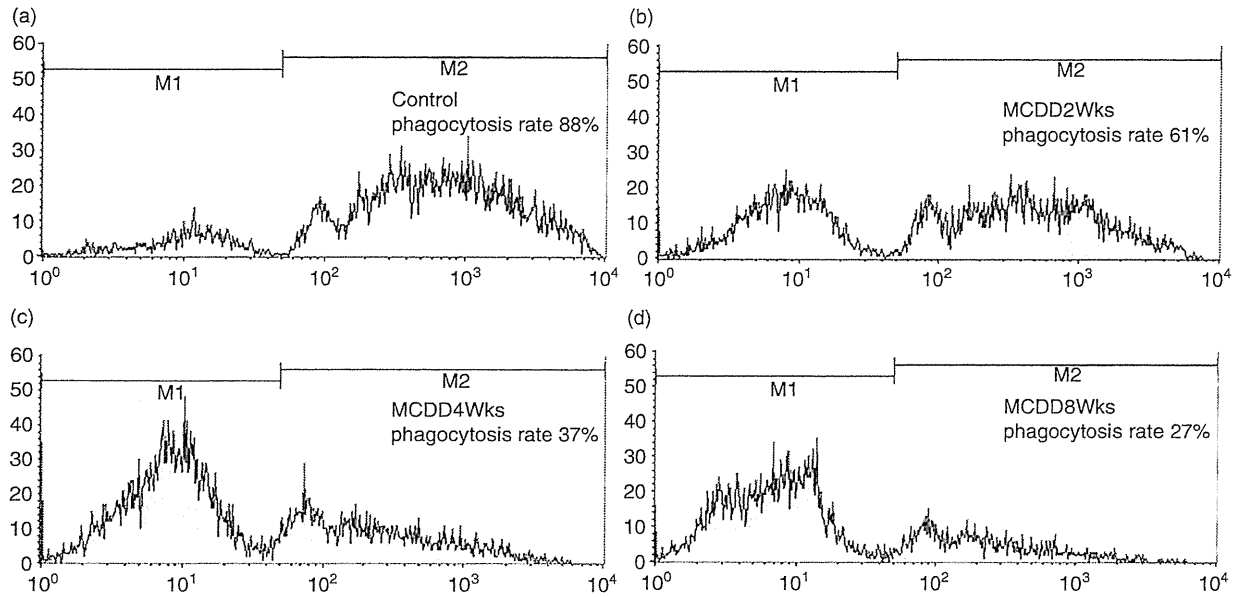

Figure 7 Flow cytometric analysis of isolated and cultured KCs after being treated with fluorescent latex beads. The vertical axis is the KC count and the horizontal axis is the fluorescent intensity. M1 is the number of KCs which did not phagocytose any beads, and M2 is the number of KCs which phagocytosed beads. The phagocytosis rate was calculated by M2/M1 + M2 (the total number of KCs). The phagocytosis rate in the control group was 88% and many latex beads were ingested, whereas the rate was 61 % in the MCDD-2wk (B), 37% in the MCDD-4wk (C) and 27% in the MCDD-8wk (D) groups, where the phagocytic capacity was decreased in proportion to the duration of MCDD administration.

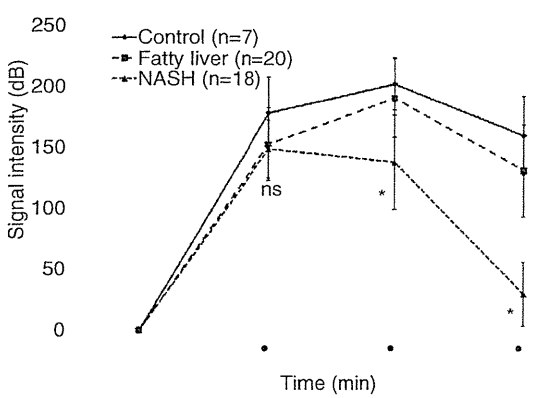

Figure 8 Parenchymal signal intensity in the early vascular phase and the delayed parenchymal phase of Levovist CEUS was evaluated in seven controls (healthy volunteers), 20 fatty liver patients and 18 NASH patients. At 1 min after the Levovist injection, the signal intensity was 178.1 ± 29.3 in the controls, 152.4 ± 30.0 in the fatty liver patients and 148.5 ± 23.6 in the NASH patients (mean ± standard deviation) and no significant differences were observed. However, at 5 and 20 min after injection, there was a significant decrease in the signal intensity in the NASH group.

REFERENCES

1 Ludwig J, Viggiano TR, McGill DB, Oh BJ. Nonalcoholic steatohepatitis: Mayo Clinic experiences with a hitherto unnamed disease. *Mayo Clin Proc* 1980; **55**: 434–8.
2 Bugianesi E, Leone N, Vanni E *et al.* Expanding the natural history of nonalcoholic steatohepatitis: from cryptogenic cirrhosis to hepatocellular carcinoma. *Gastroenterology* 2002; **123**: 134–40.
3 Shimada M, Hashimoto E, Taniai M *et al.* Hepatocellular carcinoma in patients with non-alcoholic steatohepatitis. *J Hepatol* 2002; **37**: 154–60.
4 Saadeh S, Younossi ZM, Remer EM *et al.* The utility of radiological imaging in nonalcoholic fatty liver disease. *Gastroenterology* 2002; **123**: 745–50.
5 Brunt EM, Janney CG, Di Bisceglie AM, Neuschwander-Tetri BA, Bacon BR. Nonalcoholic steatohepatitis: a proposal for grading and staging the histological lesions. *Am J Gastroentero* 1999; **94**: 2467–74.
6 Matteoni CA, Younossi ZM, Gramlich T, Boparai N, Liu YC, McCullough AJ. Nonalcoholic fatty liver disease: a spectrum of clinical and pathological severity. *Gastroenterology* 1999; **116**: 1413–9.
7 Schwenzer NF, Springer F, Schraml C, Stefan N, Machann J, Schick F. Non-invasive assessment and quantification of